International Journal of Adhesion & Adhesives 31 (2011) 88–96

Contents lists available at ScienceDirect

International Journal of Adhesion & Adhesives

journal homepage: www.elsevier.com/locate/ijadhadh

Mixed-mode fatigue behavior of degraded toughened epoxy adhesive joints

N.V. Datla [a], J. Ulicny [b], B. Carlson [b], M. Papini [c], J.K. Spelt [a,*]

[a] Department of Mechanical and Industrial Engineering, University of Toronto, 5 King's College Road, Toronto, Ont., Canada M5S 3G8
[b] GM Research and Development, 30500 Mound Road, Warren, MI 48090-9055, USA
[c] Department of Mechanical and Industrial Engineering, Ryerson University, 350 Victoria Street, Toronto, Ont., Canada M5B 2K3

ARTICLE INFO

Article history:
Accepted 14 October 2010
Available online 11 November 2010

Keywords:
Aging
Durability
Hygrothermal
Fatigue
Toughened epoxy
Open-faced

ABSTRACT

Open-faced asymmetric double cantilever beam (ADCB) specimens of toughened epoxy-aluminum adhesive joints were aged either in a constant humidity environment or a cyclically changing environment to study the mixed-mode fatigue behavior. Under constant humidity environments, the fatigue threshold strain energy release rate initially decreased with aging time until it reached a constant minimum value for long times. In contrast, the crack growth rates continued to increase with aging time. It is hypothesized that at crack growth rates close to threshold the fatigue behavior is governed by the epoxy matrix, whereas at relatively high crack growth rates the fatigue behavior is governed by the loss of the rubber toughening mechanism. Increasing the aging temperature accelerated the degradation of the joints leading to a reduction in the time to reach the constant minimum value and increased the crack growth rates.

Under a cyclic aging environment with intermittent salt spray, neither the threshold strain energy release rate nor the crack growth rates degraded until four weeks of aging. The superior fatigue performance of these joints compared to joints aged in constant humidity environments was due to the lower water concentrations in the adhesive while aging. This conclusion was supported by moisture uptake measurements of the adhesive in deionised and salt water environments that showed simple Fickian behavior at room temperature and dual-Fickian behavior at higher temperature. The salt water environment produced osmotic pressure that decreased the moisture concentration in the second stage of diffusion.

1. Introduction

Moisture can degrade adhesive joints by damaging the adhesive–adherend interfacial region or the adhesive itself. The effect of moisture on bulk epoxy adhesives depends on whether the absorbed water molecules are in a free or bound state [1]. Free water molecules plasticize and soften the adhesive, decreasing its glass transition temperature [2]; however, these effects are reversible upon drying. Bound water molecules, on the other hand, introduce irreversible damage to the adhesive by hydrolysis and chain scission [3]. Su et al. [4] studied the fatigue degradation of steel double lap joints made from several different epoxy adhesives subjected to different aging environments, and found that the adhesive that absorbed the most moisture also degraded the most. Hence, it is important to characterize the moisture diffusion behavior of an adhesive in order to understand its fatigue degradation behavior.

The fatigue behavior of fresh (undegraded) adhesive joints has been studied extensively in ambient test environments [5,6] and aggressive test environments [7–9]; however, the fatigue performance of aged adhesive joints is not well understood. Ferreira et al. [10] found that increasing the temperature of the aging environment decreased the fatigue life of composite adhesive lap joints, and related this behavior to the increased creep deformation with temperature. Lubke et al. [11] found that the fatigue behavior of epoxy-aluminum DCB joints degraded more in a high-humidity aging environment than in a natural outdoor environment; however, only mode I loading was considered. In contrast, Su et al. [4] found that the fatigue life of epoxy-steel double lap joints was more or less the same in both outdoor and high-humidity environments. In all these tests, the closed adhesive joints were first aged for relatively long periods and then fatigue tested in an ambient environment.

Closed joints are usually used in degradation studies, although they take a long time to degrade due to the length of the diffusion paths, and the degradation is non-uniform across the joint area. This non-uniform degradation makes it difficult to associate a loss of joint strength with a particular level of degradation. These limitations can be overcome using open-faced specimens that reduce the length of diffusion path to the thickness of the adhesive layer, thus producing a relatively uniform state of moisture concentration and degradation in a relatively short period of time. Open-faced specimens have previously been used to study

* Corresponding author. Tel.: +1 416 978 5435; fax: +1 416 978 7753.
E-mail address: spelt@mie.utoronto.ca (J.K. Spelt).

0143-7496/$ - see front matter © 2010 Elsevier Ltd. All rights reserved.
doi:10.1016/j.ijadhadh.2010.11.007

degradation under quasi-static loading [12–16], and the present study extends their application to cyclic loading.

This paper investigates the effect of the aging environment on the mixed-mode fatigue behavior of open-faced joints made with aluminum alloy adherends and a highly-toughened epoxy adhesive. The experiments illustrate the effects of aging time and temperature on both the fatigue threshold and crack growth rates (CGR). The experiments also compare the durability of joints aged in constant humidity and cyclic environments.

2. Experiments

2.1. Specimen preparation

Both open-faced and closed asymmetric double cantilever beam (ADCB) specimens were made using a proprietary DGEBA-based, heat-cured, rubber-toughened structural epoxy adhesive, and AA5754-O aluminum sheet with a commercial coil-coated pretreatment. Since this pretreatment could not be reliably reproduced on thicker bars, fatigue test specimens were made with 2 mm thick sheets that had been commercially pretreated. To avoid yielding of these relatively thin sheets while applying a wide range of strain energy release rates, G, the reinforcement technique discussed in Ref. [17] was used; i.e. the sheet was stiffened by bonding it to an AA6061 aluminum bar using a "reinforcing" layer of adhesive.

2.1.1. Open-faced specimens

The fatigue behavior was studied in various environments using open-faced ADCB specimens. On one side of the sheet, a 0.4 mm thick "primary" layer of adhesive was cast using a backing plate coated with polytetrafluroethylene release agent, while the other side of the sheet was reinforced by attaching it to a 12.7 mm thick P2-etched aluminum AA6061 bar using a 0.4 mm thick reinforcing layer of adhesive (Fig. 1). Since under mixed-mode loading the crack path is close to the more highly strained adherend [18], the reinforced pretreated sheet was used only as one of the adherends and the other adherend was made from a thicker aluminum bar. The desired bondline thickness was achieved by placing 0.4 mm size piano wires in both the primary and reinforcing adhesive layers. Since both the primary and reinforcing layers utilized the same adhesive, both layers could be cured in a single step using the cure profile recommend by the manufacturer; i.e., at least 30 min at 180 °C. The assembly was clamped using large binder clips (25.4 mm wide by 50.8 mm long, from ACCO brands) that were centered directly above the spacing wires in both adhesive layers to avoid an uneven bondline thickness. After curing, the backing plate was removed and the open-faced specimens (Fig. 1) were exposed to various environments for a range of times, as shown in Tables 1 and 2.

The present experiments focused on the effects of irreversible degradation by drying the aged specimens in a vacuum oven containing anhydrous calcium sulphate at 40 °C for approximately 7 days. This eliminated reversible effects such as plasticization by water molecules [13]. After drying, the complete ADCB specimen (Fig. 2) was made by bonding the primary adhesive layer of the open-faced specimen to a 25.4 mm thick P2-etched aluminum AA6061 bar using a 0.25 mm thick "secondary" layer of adhesive (the P2 etch uses sulphuric acid as described in [19]). The bondline thickness of the secondary layer was achieved by placing 0.65 mm diameter (sum of primary and secondary layer thicknesses) piano wires between the sheet and the second adherend in locations without adhesive. In order to improve the bonding between the primary and secondary adhesive layers, the degraded primary layer was sanded lightly with a 100 grit sand paper, wiped with acetone and then dried prior to the application of the secondary adhesive. After the secondary cure, the excess adhesive on the sides of the specimen was removed using a belt sander with a 120 grit sand paper and water as a coolant, followed by hand sanding with a 600 grit sand paper. A thin layer of white paper correction fluid diluted with hexane was then applied to enhance the observation of the crack tip during the fatigue testing.

2.1.2. Closed specimens

To investigate whether the presence of the secondary adhesive layer had any effect on the fatigue behavior of the adhesive primary layer, fatigue tests were also carried out on closed ADCB specimens made with a single 0.4 mm thick layer of adhesive between the sheet and second adherend. This choice of bondline thickness was made following the work of Ameli et al. [16], who found that the fracture toughness of double-layer joints depended on the thickness of the primary layer of adhesive, but not on the combined thickness of the primary and secondary layers. Therefore, the thickness of the adhesive layer in these closed specimens was chosen to be equal to the thickness of the primary layer in the open-faced specimens. The configuration of these closed specimens was the same as the open-faced specimens (Fig. 2), except for the absence of the secondary adhesive layer.

2.2. Aging conditions

Open-faced specimens were exposed to either a constant or cyclic humidity environment. Two different constant humidity environments were used: one at 40 °C and other at 60 °C, both at 95% relative humidity (RH). A constant RH was achieved by placing the specimens in air-tight plastic containers that contained a saturated salt solution of K_2SO_4. To maintain a constant temperature, the containers were placed in temperature controlled ovens.

For the cyclic environment, the conditions were varied between the ambient, humid, and dry stages in a daily cycle as shown in Table 1. During the ambient temperature stage, the specimens were exposed to a salt spray (salt fog) four times for 30 s each, as

Table 1
Stages of the cyclic aging environment.

Aging stage	Temperature and humidity	Elapsed time (h)
Ambient stage	25 ± 3 °C, 45 ± 10% RH	0–8
Humid stage	49 ± 2 °C, 100% RH	8–16
Dry stage	60 ± 2 °C, < 30% RH	16–24

Salt spray was applied in the ambient stage four times for 30 s each.

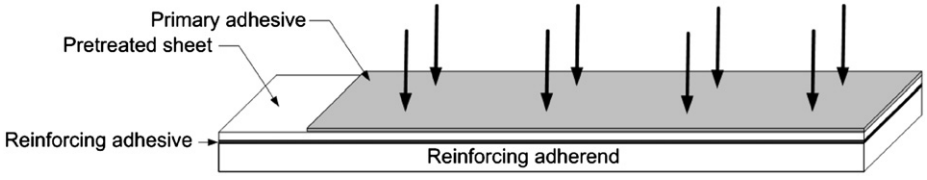

Fig. 1. Open-faced specimen used for aging. The arrows indicate the direction of moisture diffusion into the primary adhesive layer.

Table 2
SDF model parameters of the adhesive for both humid environments studied.

Environment	H_2O content (g/m^3)	Absorption					Desorption M_r (%)
		$D_1 \pm$ SD (10^{-14} m^2/s)	$D_2 \pm$ SD (10^{-14} m^2/s)	$M_{1\infty} \pm$ SD (%)	$M_\infty \pm$ SD (%)	$t_d^{1/2}$ ($s^{1/2}$)	
40 °C and 95% RH	48.0	134 ± 17	3.9 ± 0.7	3.34 ± 0.09	4.78 ± 0.15	532	1.40
60 °C and 95% RH	121.7	314 ± 25	8.9 ± 0.9	3.68 ± 0.11	6.98 ± 0.18	315	1.72

Each data point is the average of three repetitions, where SD indicates the standard deviation.

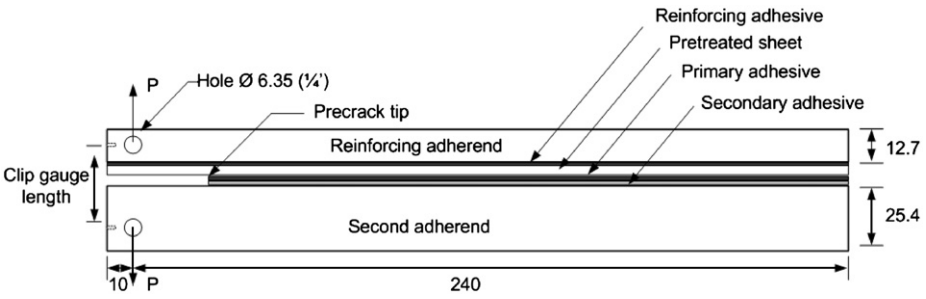

Fig. 2. Configuration of open-faced reinforced ADCB specimen after being closed (dimensions in mm, not to scale). The thickness of primary, secondary, and reinforcing adhesive layers are 0.4, 0.25, and 0.4 mm, respectively, and the thickness of the sheet is 2 mm. The location of the clip gauge is also shown. The upper adherend is the open-faced adherend shown in Fig. 1.

described in Ref. [20]. The salt solution used in the salt fog was composed of 0.9% NaCl, 0.1% $CaCl_2$, and 0.075% $NaHCO_3$ (percentages by weight).

2.3. Gravimetric measurements

The moisture uptake of the adhesive was characterized using gravimetric measurements of two sets of three adhesive wafers ($30 \times 30 \times 0.4$ mm^3) immersed in either salt water or deionised water. To ensure an initially dry state, the samples were kept in a vacuum oven at 40 °C for 7 days prior to immersion. The mass uptake was measured by weighing the wafers at fixed time intervals, after removing them from the liquids and drying them with clean tissue paper.

2.4. Fatigue tests

Fatigue testing was performed with a servo-hydraulic load frame under displacement control using a sinusoidal waveform at a frequency of 20 Hz. A constant displacement ratio (i.e. ratio of minimum to maximum displacement, $\delta_{min}/\delta_{max}$) of 0.1 was used. The testing began with the application of the highest strain energy release rate, G, which then decreased as the crack grew under constant displacement until the threshold crack growth rate of 10^{-6} mm/cycle was reached at the threshold strain energy release rate, G_{th}. The joints were enclosed in a chamber containing desiccant to maintain a room temperature dry environment ($< 10\%$ RH) while testing.

2.4.1. Crack length measurements

The crack length was measured using both optical and specimen compliance methods. Optical measurements were performed using a CCD camera mounted on a motorized linear stage. A telescopic lens attached to the camera allowed a field of view of 2 mm. To obtain clear photographs of the crack tip, load cycling was stopped and held at the mean load for 15 s every 9000 cycles. The specimen compliance was obtained from the relationship between the crack opening and the applied force during the unloading portion of the loading cycle. A clip gauge (model 3541, Epsilon Technology Corp., Jackson, WY, USA) recorded the opening displacement at the loading pins (Fig. 2). For each specimen, a polynomial relationship between the optically observed crack length and the specimen compliance was established according to ASTM E647 [21]. Using this relationship, the crack length was inferred from the continuous clip gauge compliance data, and used in all calculations of crack growth rate and G.

2.4.2. Strain energy release rate calculations

A beam-on-elastic-foundation model for unequal adherends was used to calculate G and phase angle, Ψ (defined as $\psi = \arctan\left(\sqrt{G_{II}/G_I}\right)$, where G_I and G_{II} are the mode I and mode II strain energy release rates, respectively), from the measured force and crack length [17]. The average phase angle calculated using the model was 14° for the ADCB specimen, with only a negligible change occurring as the crack grew. For example, Ψ increased by only 2° for an increase in crack length from 40 to 120 mm [17]. The phase angle in the closed open-faced joints was essentially the same as that in the closed joints that were made for comparison without the secondary adhesive (difference of less than 0.5°).

2.5. Measurement of residual adhesive thickness

To define the crack path, the thickness of the residual adhesive on some of the fracture surfaces was measured at various crack lengths on the more highly-strained adherend. The elevation datum corresponding to the steel interface was established by removing residual adhesive from a narrow region on both sides of the joint width using a solvent (mixture of methylene chloride and methyl alcohol; Glue Buster, Kosmic Surf-Pro Inc., Saint Amable, Quebec). An optical profilometer (NANOVEA ST400, Micro Photonics Inc., CA, USA) was used to make a line scan across the width of the joint with both ends on the datum regions, thereby giving the thickness of the residual adhesive layer.

3. Results and discussion

3.1. Moisture diffusion

For constant humidity environments, the water absorption of the present adhesive was previously found to be non-Fickian, with a pseudo-equilibrium state at intermediate exposure times before reaching a final saturation state [22]. The water desorption, however, was found to follow a simple Fickian trend [22]. The diffusion coefficient of the first stage and the saturated were both functions of temperature. Desorption studies showed that even after prolonged drying the adhesive retained a significant amount of water, and that the amount of retained water was proportional to the fractional mass uptake at the end of the second stage. This absorption and desorption behavior was characterized using a sequential dual-Fickian (SDF) model [22], which is described in Appendix 1.

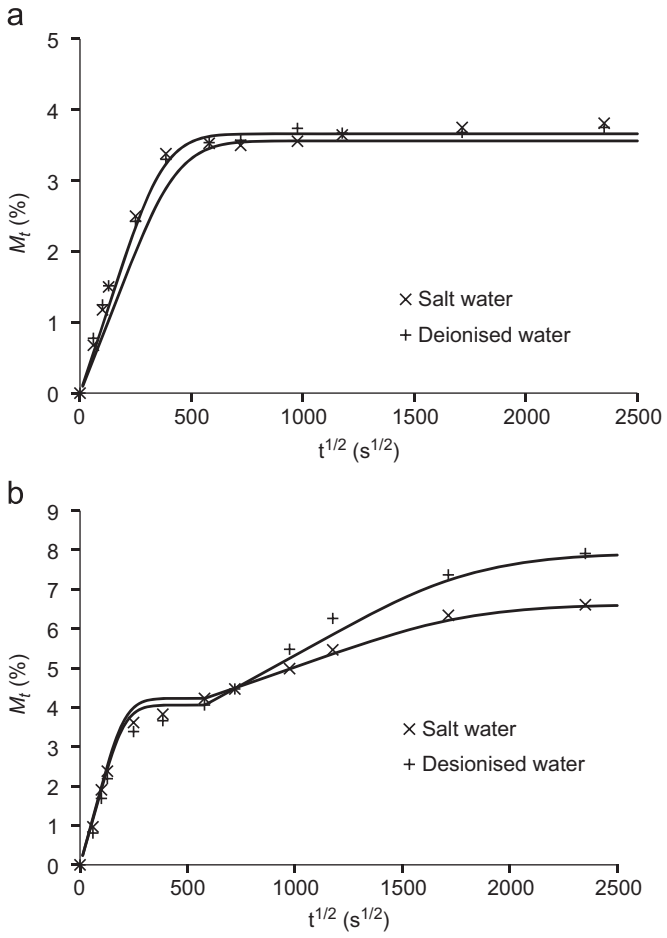

Fig. 3. Measured fractional mass uptake versus square root of time and the least-squares fits based on SDF model (Appendix) when immersed in salt water and deionised water at (a) room temperature and (b) 40 °C. Each data point is an average of three repetitions. The standard deviation in each case was approximately 2%.

Fig. 3 shows the measured moisture mass uptake and the fitted SDF model versus the square root of time for the adhesive wafers immersed in salt water and deionised water. Table 3 lists the SDF model parameters of the adhesive under both immersion conditions. At room temperature, the second diffusion mechanism was absent and the moisture uptake followed a simple Fickian behavior where both the second stage diffusion coefficient, D_2, and fractional mass uptake, M_2, were equal to zero. Furthermore, insignificant differences in the fractional mass uptake $M_{1\infty}$, and diffusion coefficient D_1, of the first stage were observed between both immersion environments (t-test, 95% confidence interval), indicating that the salt did not affect the moisture diffusion behavior at room temperature.

At 40 °C the moisture uptake followed a non-Fickian behavior, as also seen in [22]. The first stage of diffusion was similar for both immersion conditions (insignificant difference in $M_{1\infty}$ and D_1, t-test 95% confidence), whereas in the second stage the saturated mass uptake was significantly lower for the samples that were immersed in salt water than for those immersed in deionised water. This is consistent with previous work which demonstrated that increases in the concentration of the NaCl in a salt solution decreases the saturated water mass uptake into an adhesive due to osmosis [23,24]. Since the effect of the salt was observed only in the second stage of diffusion, this implies that the osmotic effects were predominant only during the second stage. Furthermore, using the same adhesive used in this study, Ameli et al. [22] showed that the diffusion mechanism in the first stage is governed by chemical interaction between the water molecules and the epoxy matrix, whereas the diffusion mechanism in the second stage is governed by relatively mobile water molecules in the adhesive. Therefore, it can be concluded that the salt water environment produces an osmotic pressure that does not affect the chemical interactions of the water molecules with the adhesive, but affects the diffusion kinetics of the mobile water molecules in the epoxy during the second stage of absorption.

3.2. Fresh open-faced specimens

To provide a baseline to which the effect of degradation can be compared, fatigue tests were conducted on fresh open-faced specimens. For these specimens, the secondary layer of adhesive of 0.25 mm thickness was applied and cured immediately after the primary layer was cured. The measured fatigue threshold strain energy release rate, G_{th}, of these joints was 125 ± 9 J/m^2 ($\pm$ standard deviation, 3 threshold measurements with each threshold from a single specimen).

The primary difference between an open-faced joint that has been closed to form an ADCB and a conventional closed joint is the presence of the secondary adhesive layer. This will increase the local

Table 3
SDF model parameters of the adhesive immersed in salt water and deionised water. Each data point is the average of three repetitions, where SD indicates the standard deviation.

Temperature (°C)	Solution	$D_1 \pm$ SD (10^{-14} m^2/s)	$D_2 \pm$ SD (10^{-14} m^2/s)	$M_{1\infty} \pm$ SD (%)	$M_\infty \pm$ SD (%)	$t_d^{1/2}$ ($s^{1/2}$)
20	Salt water	37.6 ± 5	–	3.64 ± 0.1	3.64 ± 0.1	∞
	Deionised water	30.72	–	3.53 ± 0.1	3.53 ± 0.1	∞
40	Salt water	150 ± 11	16.66 ± 5	4.22 ± 0.2	6.26 ± 0.1	580
	Deionised water	136 ± 30	16.45 ± 4	4.06 ± 0.1	5.46 ± 0.1	580

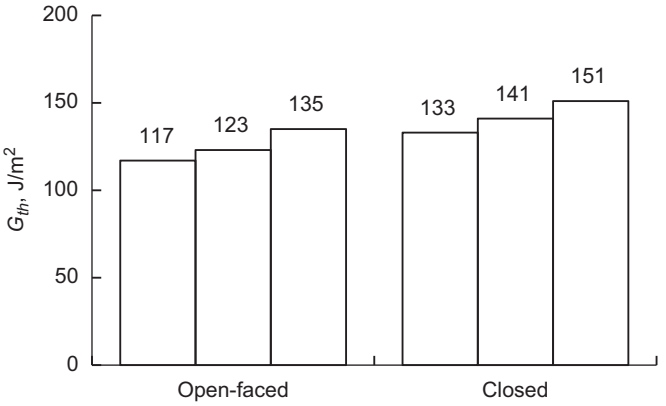

Fig. 4. Measured G_{th} of fresh closed and open-faced joints tested in a room temperature and dry air environment. The 3 test repetitions are shown in each case, with G_{th} for each specimen shown above the columns.

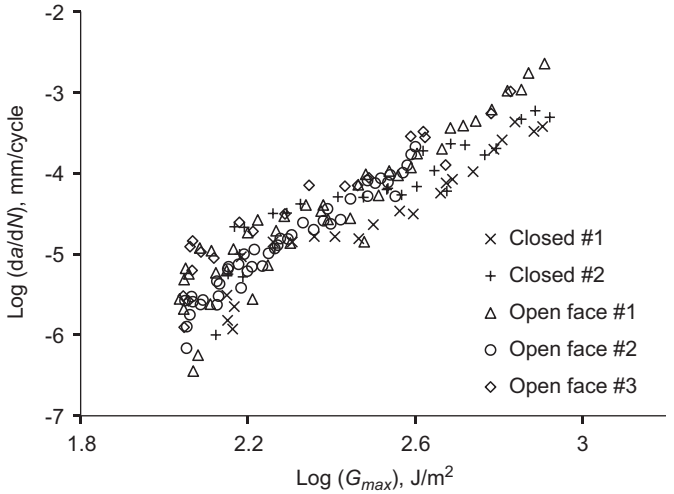

Fig. 5. The measured fatigue crack growth rate curves of unaged closed and unaged open-faced joints tested in a room temperature and dry air environment.

compliance slightly and introduce a second cure cycle to the primary adhesive layer. To investigate these effects, the fatigue behavior of fresh open-faced joints was compared to that of the conventional closed joints that were prepared with a 0.4 mm thick single layer of adhesive. Fig. 4 shows that the average G_{th} of the open-faced specimens was 9% lower than that of the closed joints, but this difference was statistically insignificant (t-test, 95% confidence level). Furthermore, Fig. 5 shows that the crack growth rate curves of both the closed and open-faced joints overlap, indicating a similar fatigue crack growth behavior. In all tests using the ADCBs made from the open-faced joints, the fatigue crack path was within the primary adhesive layer. Hence, it was concluded that the presence of the secondary adhesive layer and the second cure cycle had an insignificant effect on the fatigue behavior of the primary adhesive layer. This is consistent with the fracture test results of Ameli et al. [16], who showed an insignificant effect of a second cure cycle on the quasi-static critical strain energy release rate of conventional closed DCB joints prepared with the same adhesive used in the present study.

3.3. Aging of joints in constant Humidity environments

3.3.1. Effect of aging time and temperature on G_{th}

Fig. 6 shows the variation of G_{th} with aging time for 95% RH at 40 and 60 °C, and the average G_{th} of unaged open-faced joints. The curves

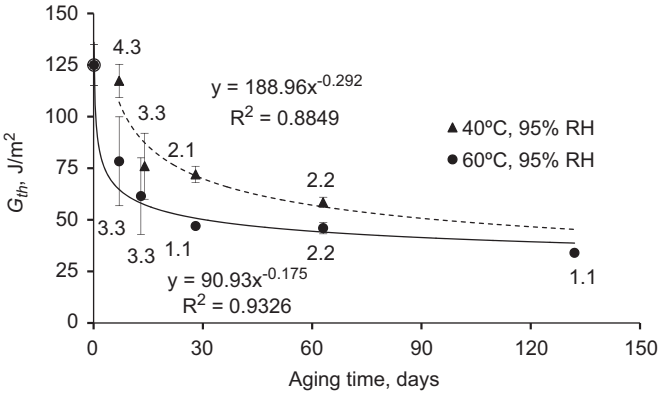

Fig. 6. Fatigue threshold vs. aging time for specimens aged under 40 °C–95% RH and 60 °C–95% RH environments. Trend lines show the exponential regression lines fit to the data. Numbers next to each data point indicate the number of thresholds reached and the number of specimens tested, respectively; these two numbers are different cases where a single specimen was used to reach two thresholds. Error bars represent the range of the measurements.

are the least-squares power function fits at each temperature. Two stages of degradation were observed in each environment. In the first stage, the threshold for the joints aged at 60 °C decreased by 65% (from 125 ± 9 to 43 ± 6) and by a lesser amount, 54% (from 125 ± 9 to 58 ± 4) for the joints aged at 40 °C. In the second stage, G_{th} remained constant at a low value with further aging. Increasing aging temperature also increased the rate at which the joints degraded and decreased the time to the onset of the second stage; i.e. approximately after two weeks at 60 °C and after one month at 40 °C.

The quasi-static fracture toughness of the adhesive used in this study was found previously to degrade in three stages [12]. Although these results were established with a different pretreatment, since the crack path was cohesive in both the present study and that of Ref. [12], the effect of pretreatment should be negligible. In the quasi-static fracture study of ref. [12], the first two stages of degradation were similar to those described above, but during the third stage, after very long aging times, the critical quasi-static fracture toughness decreased further. In the present study, it was not possible to determine whether a third stage of degradation might exist for specimens aged over 6 months at 60 °C and 95% RH, because fatigue cracks grew in the reinforcing adhesive layer rather than in the primary adhesive layer for these long exposure times. This occurred because moisture diffused into the reinforcing layer from the exposed sides of the open-faced joint, reaching moisture concentrations of 3.8% at centre and 6.98% at the edges of the reinforcing layer. This absorbed moisture was not completely desorbed while drying the primary adhesive layer, and probably caused damaging internal stresses to develop during the secondary cure cycle. Hence, the reinforcing layer was weaker than the primary layer. This limitation could have been avoided by applying an additional sealant to the sides of the open-faced specimens.

3.3.2. Effect of aging time and temperature on crack growth behavior

Fig. 7 shows the scatter in the crack growth rate curves of specimens aged for two months at 40 and 60 °C. It can be seen that the scatter is slightly larger in the degraded specimens than in the fresh joints (Fig. 5). Fig. 8 shows the variation in the crack growth rate curves with aging time at 40 and 60 °C, respectively. At shorter aging times (up to one month at 40 °C and one week at 60 °C), insignificant differences were observed between the crack growth rate curves of fresh and aged joints. However, as the aging time increased, the crack growth rates at a given applied G_{max} increased (i.e. the curves for the aged joints began to shift upward). This happened sooner and to a large extent at 60 °C than at 40 °C,

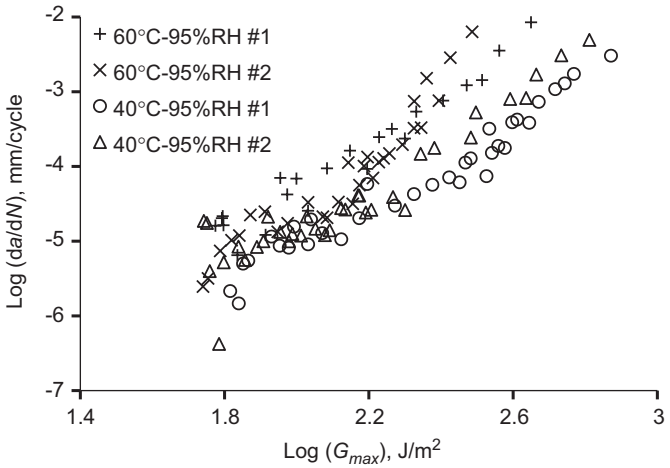

Fig. 7. Repetitions of the measured fatigue crack growth rate curves of specimens aged for 60 days at 40 °C–95% RH and 60 °C–95% RH. Two specimens aged at each condition.

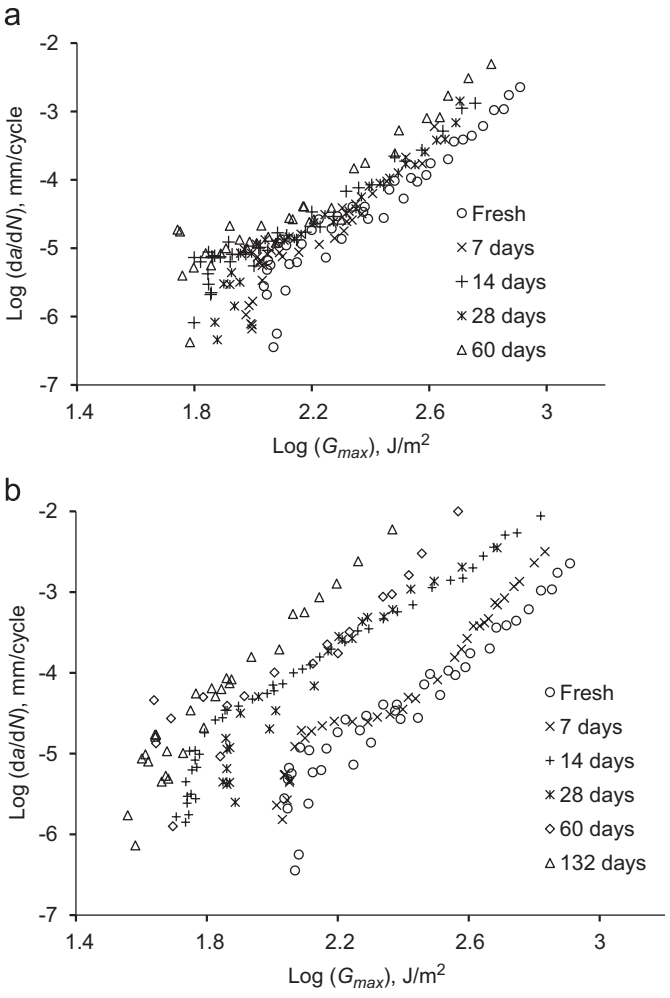

Fig. 8. Measured fatigue crack growth rate curves of specimens aged at (a) 40 °C–95% RH and (b) 60 °C–95% RH. Aging time in days is given in the legend.

reflecting the accelerating effect of temperature on fatigue degradation. This is illustrated further in Fig. 9, which shows that the differences in the crack growth rates at the two aging temperatures were insignificant after the first week of aging, and grew after that. For example, at an applied G_{max} of 250 J/m^2, the crack speeds were 0.4, 5.8, 8.5, and 7.9 times greater at 60 °C than at 40 °C for aging times of one week, two weeks, one month and two months, respectively.

The threshold and crack growth rate behaviors were affected differently by degradation. At 60 °C, G_{th} decreased to a saturated level after two weeks of aging, whereas the fatigue crack growth rate continued to decrease until after 4 months of aging. It is hypothesized that the fatigue failure mechanisms near the threshold are different from those at higher crack growth rates. Indeed, using a rubber toughened epoxy adhesive, Azimi et al. [25] showed that adhesive toughening mechanisms were absent at crack growth rates close to the threshold, and that the fatigue behavior was similar to an unmodified epoxy. Hence, it is likely that the continuing increase in the crack growth rate with aging time was related to the loss of the toughening mechanisms from the rubber particles, and the decrease in G_{th} was related to the degradation of the epoxy matrix.

3.3.3. *Effect of aging time and temperature on crack path*

Fig. 10 shows that the crack paths in both the unaged and aged joints were cohesive at all crack growth rates. Furthermore, the thickness of the residual adhesive on the more highly-strained open-faced adherend decreased monotonically with decreasing crack growth rate (decreasing G_{max}) in all specimens (Fig. 11). In [17], a similar trend was explained in terms of the decreasing size of the plastic zone at the tip of the crack as the applied G decreased. Assuming that the average crack path tends toward the centre of the plastic zone, the residual adhesive thickness will also decrease as the applied G decreases and the crack slows. Related to this argument, Fig. 11 also shows that at a relatively high crack growth rates, the thickness of the residual adhesive decreased with aging due to the lower associated G levels and the resulting smaller crack tip plastic zones. The residual adhesive thickness in the threshold region did not change appreciably with aging time.

3.4. *Aging of joints in cyclic environment*

Figs. 12 and 13 show the G_{th} and crack growth rate curves of open-faced joints aged in the cyclic environment for two and four weeks, respectively. Statistically insignificant differences were observed in G_{th} and the slope of the linear Paris regions of the fresh and aged joints (t-test, 95% confidence), indicating that the joints were undegraded even after four weeks of aging in the cyclic environment. In contrast, Figs. 6 and 8 show that, for the same aging time, the joints degraded significantly in the constant humidity environments. For example, after 4 weeks of aging, G_{th} of the joints aged in the constant humidity environment decreased by 62% (from 125 ± 10 to 47 J/m^2) at 60 °C–95% RH and by 42% (from 125 ± 10 to 72 ± 0034 J/m^2) at 40 °C–95% RH, whereas G_{th} of the joints aged in the cyclic humidity environment increased slightly by 3% (from 125 ± 9 to 128 ± 11 J/m^2). It was therefore hypothesized that the moisture concentration in the specimens aged in the cyclic environment was below that in the specimens aged in the constant humidity environments. To investigate this hypothesis, a two-dimensional finite element model was used to estimate the moisture concentration in the adhesive for specimens aged in the cyclic environment.

The cross-section (0.4×18 mm^2) of the adhesive layer was modeled using a total of 192 4-node thermal PLANE55 elements (ANSYS 12.0, Canonsburg, PA, USA), used with a thermal—diffusion analogy. The top surface and the sides of the adhesive were assumed to be at the saturated moisture concentration, and moisture transfer was prevented on the bottom surface. To simplify the model, water diffusion was approximated using Fick's law rather than the more accurate dual-Fickian mode. Table 4 shows

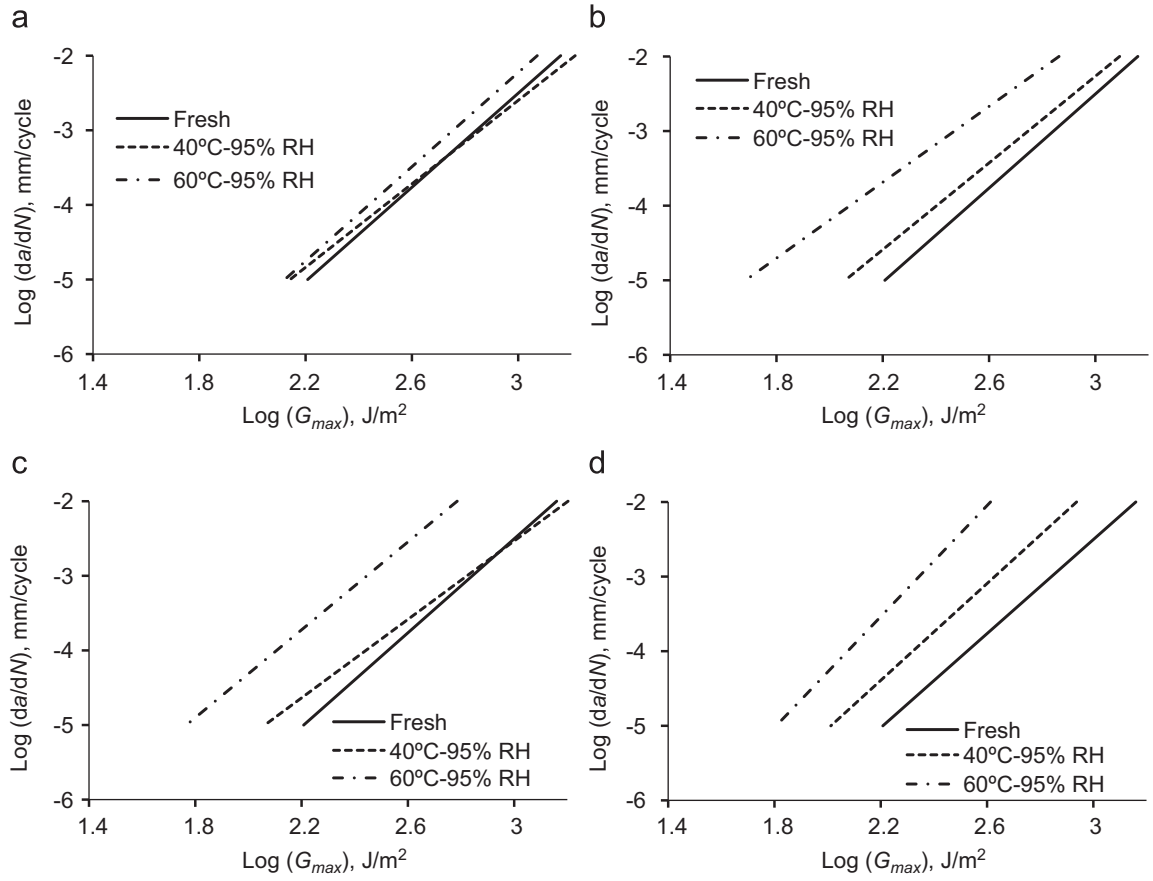

Fig. 9. Effect of aging temperature on the crack growth rate curves for specimens aged for (a) 1 week, (b) 2 weeks, (c) 1 month, and (d) 2 months. Each line is the least-squares fit to the linear Paris region of the crack growth curves shown in Fig. 8.

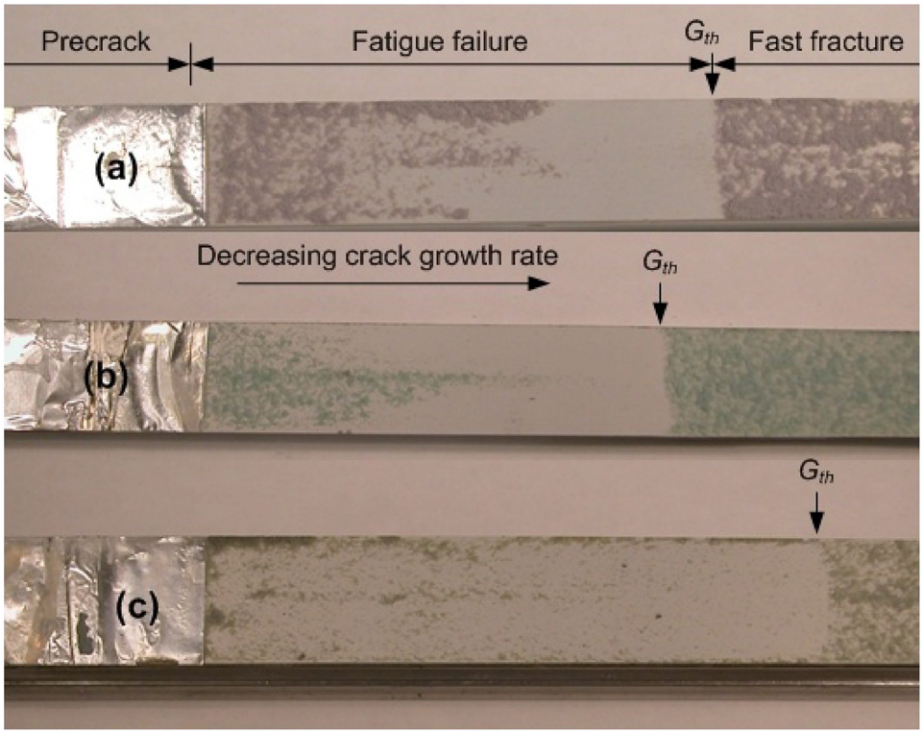

Fig. 10. Fracture surfaces on the more highly-strained (reinforced) adherend for: (a) unaged joint, (b) 2 weeks aged at 60 °C–95% RH, and (c) 4 months aged at 60 °C–95% RH.

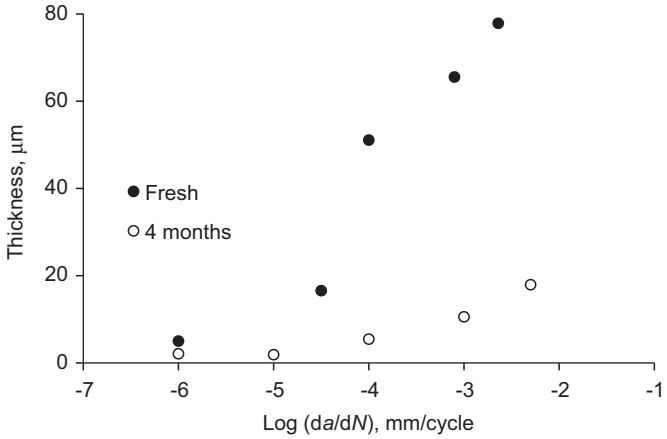

Fig. 11. Thickness of the residual adhesive on the fracture surface of the more highly-strained adherend as a function of crack growth rate for a fresh joint and a joint aged for four months at 60 °C–95% RH.

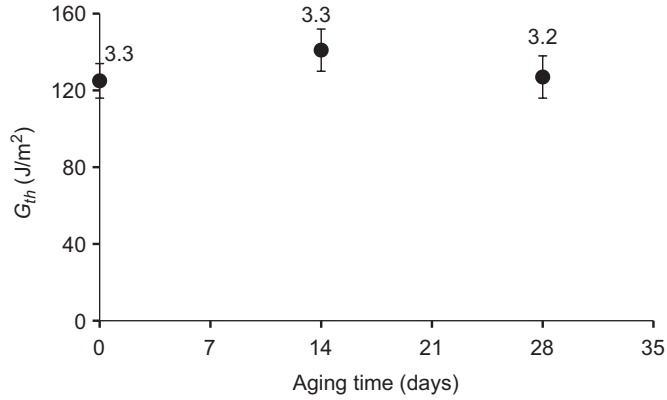

Fig. 12. Fatigue threshold versus aging time for open-faced specimens aged in the cyclic environment. Numbers next to each data point indicate the number of thresholds reached and the number of specimens tested, respectively; these two numbers are different cases where a single specimen was used to reach two thresholds. The error bars show ±1 standard deviation.

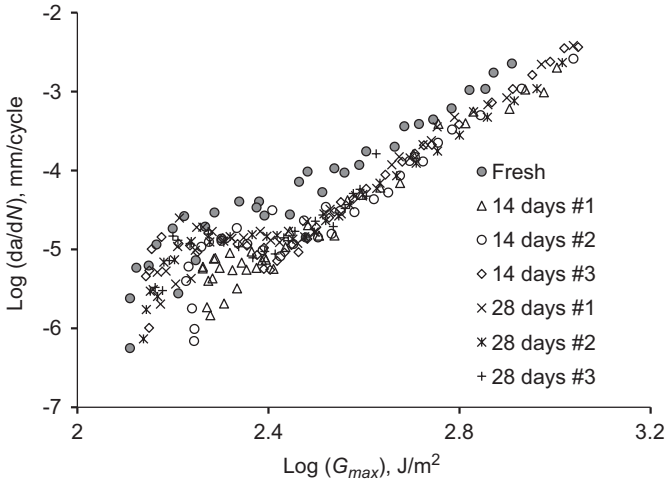

Fig. 13. Crack growth rates versus applied G_{max} for specimens aged in the cyclic environment. Three specimens at each aging condition.

the adhesive diffusion parameters that were used for the different stages of the cyclic aging environment of Table 1. These diffusion parameters were taken to be those measured in [22], for the same

Table 4
Moisture diffusion parameters of the adhesive used in the finite element model. Data is from [22].

Aging stage	D (10^{-14} m^2/s)	M_∞ (%)
Ambient stage	45	1.78
Humid stage	207	6.67
Dry stage	271	1.62

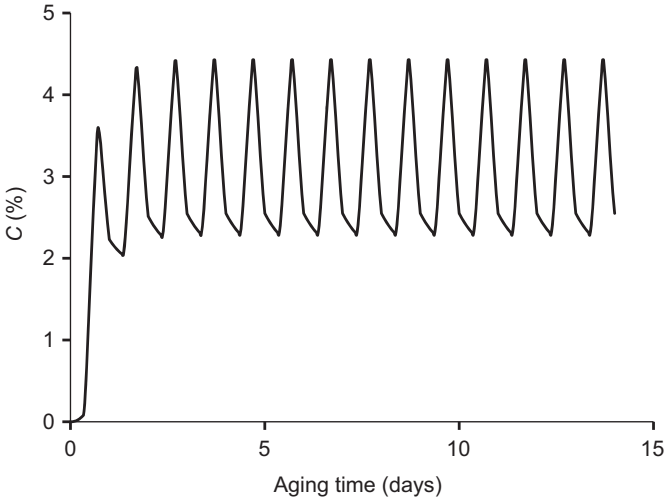

Fig. 14. Moisture concentration (mass of water per unit mass of adhesive) profile at the adherend–adhesive interface of the open-faced specimen exposed to the cyclic environment.

adhesive used in the present study. Mesh refinement did not change the moisture concentration at the adhesive–adherend interface by more than 0.1%.

Fig. 14 shows the finite element model predictions of the moisture concentration versus aging time at the adhesive–adherend interface, which is the locus of failure in the threshold region. It can be seen that the moisture concentration at this interface reached a cyclic equilibrium, varying between 2.2% and 4.3% after the third day of aging. These concentrations were significantly below the saturated moisture concentrations of 4.8% and 7.0% at 40 and 60 °C aging environments, respectively. Moreover, these levels of water uptake would not increase with longer exposure to the cyclic environment since drying and absorption reached a cyclic equilibrium. This explains why the fatigue behavior of the joints aged in the cyclic environment would be superior to that of joints aged in the constant humidity environments. Moreover, the intermittent salt spray application did not appear to accelerate the degradation process, probably because of the decreased saturated moisture concentration in the adhesive in the presence of the salt solution. Finally, the thermal cycling aspect of this accelerated aging test did not seem to produce any measureable effect.

4. Conclusions

The mixed-mode fatigue behavior of degraded toughened epoxy-aluminum adhesive joints was studied using open-faced ADCB specimens. Both constant humidity environments and cyclic environments were studied. In constant humidity environments, the fatigue threshold and crack growth rate behavior were affected differently. The fatigue threshold strain energy release rate, G_{th},

decreased from an undegraded value to a constant minimum value that did not change even after prolonged aging. In contrast, the crack growth rates continued to increase with aging time, showing no tendency to reach a limiting value. It was hypothesized that the continuing increase in the crack growth rate with aging time was related to the loss of the rubber toughening mechanism, and that the decrease in G_{th} was related to the degradation of the epoxy matrix. Increasing the aging temperature accelerated the rate at which G_{th} decreased from its initial value. The crack paths remained cohesive in the adhesive layer in all of the experiments, with the residual adhesive thickness on the more highly-strained adherend decreasing as the crack growth rate (or applied G) decreased.

For joints aged in the cyclically changing environment with intermittent salt spray, neither G_{th} nor the crack growth rates degraded until after four weeks of aging. The superior fatigue performance of these joints compared to joints aged in constant humidity environments was due to the lower equilibrium water concentrations in the adhesive, which were modeled using the finite element method. This was supported by moisture uptake measurements of the adhesive in deionised and salt water environments which showed that the diffusion was simple Fickian at room temperature and dual-Fickian at the higher temperatures. The salt spray produced an osmotic pressure that affected the diffusion kinetics of the mobile water molecules in the epoxy during absorption.

Acknowledgments

The work was supported by General Motors of Canada Ltd., the Natural Sciences and Engineering Research Council of Canada, and the Ontario Centres of Excellence. The authors would like to acknowledge GM R&D, Warren, for providing facilities for intermittent salt-spray aging.

Appendix A. Moisture diffusion

The sequential dual-Fickian (SDF) model was used to determine the moisture concentration at any time, t, and distance, x, from the boundary by [22]:

$$C(x,\ t) = \left(1-\frac{4}{\pi}\sum_{n=0}^{\infty}\frac{(-1)^n}{2n+1}\exp\left(\frac{-D_1(2n+1)^2\pi^2 t}{4h^2}\right)\cos\frac{(2n+1)\pi x}{2h}\right) \times C_{1\infty} + \phi(t-t_d)\times\left(1-\frac{4}{\pi}\sum_{n=0}^{\infty}\frac{(-1)^n}{2n+1} \times\exp\left(\frac{-D_2(2n+1)^2\pi^2(t-t_d)}{4h^2}\right)\cos\frac{(2n+1)\pi x}{2h}\right)\times C_{2\infty} \quad (A.1)$$

where $C_{1\infty}$ and $C_{2\infty}$ are the saturated concentrations of the first and second diffusion mechanisms such that $C_{1\infty}+C_{2\infty}=C_{\infty}$, where C_{∞} is the total saturation concentration. D_1 and D_2 are the diffusion coefficients of the first and second moisture uptake mechanisms, respectively. t_d is the time at which the transition from the first diffusion mechanism to the second one occurs, and $\Phi(t)$ is the aviside step function which is equal to zero for negative values and equal to one for positive values.

Integrating Eq. (A.1) over the spatial variable, the fractional mass uptake, M_t for the SDF model at any time t is given by

$$M_t = \left(1-\frac{8}{\pi^2}\sum_{n=0}^{\infty}\frac{1}{(2n+1)^2}\exp\left(\frac{-D_1(2n+1)^2\pi^2 t}{4h^2}\right)\right)\times M_{1\infty} + \phi(t-t_d) \times\left(1-\frac{8}{\pi^2}\sum_{n=0}^{\infty}\frac{1}{(2n+1)^2}\exp\left(\frac{-D_2(2n+1)^2\pi^2(t-t_d)}{4h^2}\right)\right)\times M_{2\infty} \quad (A.2)$$

where $M_{1\infty}$ and $M_{2\infty}$ correspond to the first and second uptakes, respectively, and $M_{1\infty}+M_{2\infty}=M_{\infty}$. The fractional mass uptake at any time t, M_t was determined experimentally using gravimetric measurements according to

$$M_t = \frac{W_t - W_i}{W_i}\times 100\% \quad (A.3)$$

where W_i and W_t are the sample weights before any exposure and after an exposure time of t, respectively. The model has 5 parameters: D_1, D_2, $C_{1\infty}$, $C_{2\infty}$ and t_d. Further details on calculating the model parameters are given in Ref. [22].

References

[1] LaPlante G, Ouriadov AV, Lee-Sullivan P, Balcom BJ. Anomalous moisture diffusion in an epoxy adhesive detected by magnetic resonance imaging. J Appl Polym Sci 2008;109:1350–9.
[2] Lin KF, Yeh RJ. Moisture absorption behavior of rubber-modified epoxy resins. J Appl Polym Sci 2002;86:3718–24.
[3] Xian G, Karbhari VM. DMTA based investigation of hygrothermal ageing of an epoxy system used in rehabilitation. J Appl Polym Sci 2007;104:1084–94.
[4] Su N, Mackie RI, Harvey WJ. The effects of aging and environment on the fatigue life of adhesive joints. Int J Adhes Adhes 1992;12:85–93.
[5] Johnson WS, Mall S. A fracture mechanics approach for designing adhesively bonded joints. In: Johnson WS, editor. Delamination and debonding of materials, ASTM STP 876. American Society for Testing and Materials; 1985. p. 189–99.
[6] Mall S, Johnson WS. Characterization of mode I and mixed-mode failure of adhesive bonds between composite adherends. In: Whitney JM, editor. Composite materials: testing and design, ASTM STP 893. American Society for Testing and Materials; 1986. p. 322–334.
[7] Harris JA, Fay PA. Fatigue life evaluation of structural adhesives for automotive applications. Int J Adhes Adhes 1992;12:9–18.
[8] Fernando M, Harjoprayitno WW, Kinloch AJ. A fracture mechanics study of the influence of moisture on the fatigue behaviour of adhesively bonded aluminium-alloy joints. Int J Adhes Adhes 1996;16:113–9.
[9] Briskham P, Smith G. Cyclic stress durability testing of lap shear joints exposed to hot-wet conditions. Int J Adhes Adhes 2000;20:33–8.
[10] Ferreira JAM, Reis PN, Costa JDM, Richardson MOW. Fatigue behaviour of composite adhesive lap joints. Compos Sci Technol 2002;62:1373–9.
[11] Lubke KA, Butkus LM, Johnson WS. Effect of environment on fracture toughness and debond growth of aluminum/FM®73/boron-epoxy adhesively bonded joints. J Compos Technol Res 2001;23:42–9.
[12] Ameli A, Papini M, Spelt JK. Fracture R-curve of a toughened epoxy adhesive as a function of irreversible degradation. Mater Sci Eng A 2010;527:5105–14.
[13] Wylde JW, Spelt JK. Measurement of adhesive joint fracture properties as a function of environmental degradation. Int J Adhes Adhes 1998;17:237–46.
[14] Moidu A, Sinclair AN, Spelt JK. Adhesive joint durability assessed using open-faced peel specimens. J Adhes 1998;65:239–57.
[15] Loh WK, Crocombe AD, Abdel Wahab MM, Ashcroft IA. Environmental degradation of the interfacial fracture energy in an adhesively bonded joint. Eng Fract Mech 2002;69:2113–28.
[16] Ameli A, Papini M, Spelt JK. Hygrothermal degradation of two rubber-toughened epoxy adhesives: application of open-faced fracture tests. Int J Adhes Adhes, in press, doi:10.1016/j.ijadhadh.2010.10.001.
[17] Datla NV, Papini M, Schroeder JA, Spelt JK. Modified DCB and CLS specimens for mixed-mode fatigue testing of adhesively bonded thin sheets. Int J Adhes Adhes 2010;30:439–47.
[18] Hutchinson JW, Suo Z. Mixed-mode cracking in layered materials. Adv Appl Mech 1992;29:63–191.
[19] ASTM D2651. Standard guide for metal surfaces for adhesive bonding. West Conshohocken (PA): ASTM International, 2001.
[20] Rebak RB, Aprigliano LF, Daniel Day S, Farmer JC. Salt fog testing iron-based amorphous alloys. Mater Res Soc Symp Proc 2007;985.
[21] ASTM. Standard test method for measurement of fatigue crack growth rates, E647, 2000.
[22] Ameli A, Datla NV, Papini M, Spelt JK. Hygrothermal properties of highly toughened epoxy adhesives, J Adhes 2010;86:698–725.
[23] Kahraman R, Al-Harti M. Moisture diffusion into aluminum powder-filled epoxy adhesive in sodium chloride solutions. Int J Adhes Adhes 2005;25:337–41.
[24] Tai RCL, Szklarska-Smialowska Z. Effect of fillers on the degradation of automotive epoxy adhesives in aqueous solutions. J Mater Sci 1993;28:6199–204.
[25] Azimi HR, Pearson RA, Hertzberg RW. Fatigue of rubber-modified epoxies: effect of particle size and volume fraction. J Mater Sci 1996;31:3777–89.